CORE
Metadata, citation and similar papers at core.ac.uk
Provided by RERO DOC Digital Library
which should be cited to refer to this work.

Is the proton radius a player in the redefinition of the International System of Units?

By F. Nez[1,*], A. Antognini[2], F. D. Amaro[3], F. Biraben[1], J. M. R. Cardoso[3], D. Covita[3], A. Dax[4], S. Dhawan[4], L. Fernandes[3], A. Giesen[5], T. Graf[6], T. W. Hänsch[2], P. Indelicato[1], L. Julien[1], C.-Y. Kao[7], P. E. Knowles[8], E. Le Bigot[1], Y.-W. Liu[7], J. A. M. Lopes[3], L. Ludhova[8], C. M. B. Monteiro[3], F. Mulhauser[8], T. Nebel[2], P. Rabinowitz[9], J. M. F. dos Santos[3], L. Schaller[8], K. Schuhmann[5], C. Schwob[1], D. Taqqu[10], J. F. C. A. Veloso[3], F. Kottmann[11] and R. Pohl[2]

[1]*Laboratoire Kastler Brossel, ENS, UPMC and CNRS, 4 place Jussieu, 75252 Paris Cedex 05, France*
[2]*Max Planck Institut für Quantenoptik, 85748 Garching, Germany*
[3]*Departamento de Fisica, Universidade de Coimbra, 3000 Coimbra, Portugal*
[4]*Physics Department, Yale University, New Haven, CT 06520, USA*
[5]*Dausinger and Giesen GmbH, Rotebühlstraße 87, 70178 Stuttgart, Germany*
[6]*Institut für Strahlwerkzeuge, Universität Stuggart, 70569 Stuggart, Germany*
[7]*Physics Department, National Tsing Hua University, Hsinchu 300, Taiwan*
[8]*Département de Physique, Université de Fribourg, 1700 Fribourg, Switzerland*
[9]*Department of Chemistry, Princeton University, Princeton, NJ 08544, USA*
[10]*Paul Scherrer Institut, 5232 Villigen-PSI, Switzerland*
[11]*Institut für Teilchenphysik, ETH Zürich, 8093 Zürich, Switzerland*

It is now recognized that the International System of Units (SI units) will be redefined in terms of fundamental constants, even if the date when this will occur is still under debate. Actually, the best estimate of fundamental constant values is given by a least-squares adjustment, carried out under the auspices of the Committee on Data for Science and Technology (CODATA) Task Group on Fundamental Constants. This adjustment provides a significant measure of the correctness and overall consistency of the basic theories and experimental methods of physics using the values of the constants obtained from widely differing experiments. The physical theories that underlie this adjustment are assumed to be valid, such as quantum electrodynamics (QED). Testing QED, one of the most precise theories is the aim of many accurate experiments. The calculations and the corresponding experiments can be carried out either on a boundless system, such as the electron magnetic moment anomaly, or on a bound system, such as atomic hydrogen. The value of fundamental constants can be deduced from the comparison of theory and experiment. For example, using QED calculations, the value of the fine structure

*Author for correspondence (francois.nez@spectro.jussieu.fr).

One contribution of 15 to a Discussion Meeting Issue ‘The new SI based on fundamental constants’.

http://doc.rero.ch

constant given by the CODATA is mainly inferred from the measurement of the electron magnetic moment anomaly carried out by Gabrielse's group. (Hanneke *et al.* 2008 *Phys. Rev. Lett.* **100**, 120801) The value of the Rydberg constant is known from two-photon spectroscopy of hydrogen combined with accurate theoretical quantities. The Rydberg constant, determined by the comparison of theory and experiment using atomic hydrogen, is known with a relative uncertainty of 6.6×10^{-12}. It is one of the most accurate fundamental constants to date. A careful analysis shows that knowledge of the electrical size of the proton is nowadays a limitation in this comparison. The aim of muonic hydrogen spectroscopy was to obtain an accurate value of the proton charge radius. However, the value deduced from this experiment contradicts other less accurate determinations. This problem is known as the proton radius puzzle. This new determination of the proton radius may affect the value of the Rydberg constant R_∞. This constant is related to many fundamental constants; in particular, R_∞ links the two possible ways proposed for the redefinition of the kilogram, the Avogadro constant N_A and the Planck constant h. However, the current relative uncertainty on the experimental determinations of N_A or h is three orders of magnitude larger than the 'possible' shift of the Rydberg constant, which may be shown by the new value of the size of the proton radius determined from muonic hydrogen. The proton radius puzzle will not interfere in the redefinition of the kilogram. After a short introduction to the properties of the proton, we will describe the muonic hydrogen experiment. There is intense theoretical activity as a result of our observation. A brief summary of possible theoretical explanations at the date of writing of the paper will be given. The contribution of the proton radius puzzle to the redefinition of SI-based units will then be examined.

Keywords: proton radius; muonic hydrogen; Rydberg constant; Planck constant; Avogadro constant

http://doc.rero.ch

1. The proton

Even though the proton is one of the most abundant constituents of the visible Universe, some of its properties are not well known. The study of its properties is important for our deep understanding of matter. The proton is made up of three valence quarks (up, up, down), held together by strong interactions. *Ab initio* calculations can be made on this structure using quantum chromodynamics (QCD) theory.

An important step has been the calculation of the mass of the proton using QCD theory with a relative uncertainty better than 4 per cent [1,2]. Experimentally, the absolute mass of the proton is known with a relative uncertainty of 5×10^{-8} [3].

The *ab initio* calculation of the spin of the proton (i.e. 1/2) has also been undertaken. The present state of the problem is known as the 'spin crisis' [4]. This refers to the experimental finding that only a small contribution of the spin of the proton seems to be carried by the quarks [5–7]. Indeed, the study of the spin structure of the nucleon is an important task in particle physics, either theoretically [8] or experimentally [9].

Some attempts have also been made to estimate the proton charge radius with QCD theory. Some values of r_p have been published [10,11]. New and more

reliable values of the proton radius should be available in the future as calculation capabilities are increasing with time.

2. Experimental determinations of the proton charge radius

(*a*) *Scattering experiments*

In fact, the best knowledge of the proton charge radius comes from experiments. First determinations were given by electron–proton elastic scattering experiments. The principle of these experiments is to measure the differential cross section of a scattered electron beam sent onto a thin hydrogen (H_2) target. The relevant parameter is the space-like momentum transfer $-Q^2$. The proton mean square charge radius is given by the slope of the Sachs form factor (G_E) of the proton at $Q^2 = 0$,

$$\langle r_{\mathrm{p}}^2 \rangle = -6 \left. \frac{\partial G_E(Q^2)}{\partial Q^2} \right|_{Q^2=0}. \tag{2.1}$$

The proton radius is defined as

$$r_{\mathrm{p}} = \sqrt{\langle r_{\mathrm{p}}^2 \rangle}. \tag{2.2}$$

The main contribution to r_{p} comes from low-momentum measurements. Even if conceptually the experiment is simple, practically it is not. The space-like momentum transfer cannot be made arbitrarily small. The electron must cross the target in which a single elastic scatter has to occur. Measurements near to $Q^2 = 0$ must not be affected by the direct electron beam. Therefore, the proton radius can only be obtained from extrapolation of the differential cross section at $Q^2 = 0$. This extrapolation is strongly model dependent. The first determination of r_{p} was obtained in 1955 [12]. In the 1980s, an experiment was specially designed in Mainz to obtain an accurate value of r_{p} from low-momentum transfers. The analysis of the data obtained in Mainz gives $r_{\mathrm{p}} = 0.862(12)$ fm [13], which is in strong disagreement with an accurate previous determination [14]. During the 2000s, no new scattering experiment were carried out at low-momentum transfers. All the different values of r_{p} which have been published come from a re-analysis of the low-momentum scattering data, associated or not to high-momentum scattering data (e.g. [15,16]). The re-analysis considered by the Committee on Data for Science and Technology (CODATA) task group has been obtained by Sick [17]. This work takes into account the world data on elastic electron–proton scattering, the coulomb distortion, and uses a parametrization that allows us to deal properly with the higher moments. In the 2000s, a sophisticated experiment was carefully designed at Mainz to measure r_{p} accurately [18]. Taking advantage of three high-resolution spectrometers, it was possible to measure the elastic electron–proton scattering cross section with a statistical precision of better than 0.2 per cent. The value of r_{p} published in 2010, deduced from an analysis done in Mainz with their data, is 0.879(8) fm [19]. Another value of r_{p} from scattering experiments has been published very recently [20]. This value of the proton radius is deduced from the global analysis reported in Arrington *et al.* [21], in which the new measurements done at 'high' Q^2 [20] are included.

http://doc.rero.ch

(*b*) *Hydrogen spectroscopy*

At short distance, the coulombian electrostatic potential is 'shielded by the finite size of the proton'. Consequently, the energy levels of atomic hydrogen are slightly shifted. Therefore, a value of r_p can be obtained from high-resolution spectroscopy of hydrogen. A simplified but powerful analysis of the main hydrogen data has been presented in de Beauvoir *et al.* [22] by using only the most accurate experimental data: the frequency of the 1S–2S transition measured in Garching, Germany [23], the 2S–8S/8D transitions measured in Paris, France [24], and the $1/n^3$ dependence of quantum electrodynamics (QED) corrections [25,26] (where n is the principal quantum number of hydrogen theory). A precise value of the 1S Lamb shift of hydrogen can be extracted from a proper linear combination of these three quantities. Assuming the exactness of QED calculations, an accurate value of r_p can be deduced. A complete analysis of all the spectroscopic measurements is also regularly done by the CODATA Task Group on Fundamental Constants (e.g. [3]). The last resulting spectroscopic value of r_p was 0.8760(78) fm.

(*c*) *Muonic hydrogen spectroscopy*

The aim of the muonic hydrogen spectroscopy of the 2S–2P splitting was to determine the proton radius more accurately. Muonic hydrogen (μ-p) is an exotic atom in which the muon (μ^-) replaces the electron 'orbiting around' the proton in normal atomic hydrogen. Like the electron, the muon is a lepton, but it is 207 times heavier and its lifetime is only 2.2 μs. Because of the mass dependence, the Bohr radius of μ-p is around 200 times smaller than that of electronic hydrogen, and the sensitivity to the finite size of the proton is then largely enhanced. The contribution owing to the finite size of the proton is around 2 per cent to the 2S–2P splitting of muonic hydrogen, whereas it is only 1.4×10^{-4} for the $2S_{1/2}$–$2P_{1/2}$ of electronic hydrogen. Another important issue in the comparison between muonic and electronic hydrogen is the vacuum polarization, which is the dominant contribution to the 2S–2P splitting of μ-p. As the Bohr radius is 200 times smaller, the overlap of S state wave functions with the distribution of virtual electron–positron pairs is more important; consequently, the contributions of the vacuum polarization corrections are larger. The wavelength of the 2S–2P transition in μ-p is 6 μm and the oscillator strength is 10^{-7} of that of electronic hydrogen. Moreover, the population of muonic hydrogen in the 2S state is small. Because of those considerations this experiment has been really challenging.

3. Muonic hydrogen experiment

(*a*) *Principle of the experiment*

The principle of the experiment has been described in many papers [27].

Let us recall the main step. The muon (μ^-) beam is sent into a H_2 gas target. Muonic hydrogen atoms are formed at the principal quantum number of around $n = 14$: the muon goes from the continuum to a bound state by ejection of an Auger electron. Subsequently, the H_2 molecule breaks up and the muonic cascade of the neutral μ-p atom begins. Radiative and collisionally induced de-excitation processes bring it down to the 2S or 1S state within a few nanoseconds (figure 1).

http://doc.rero.ch

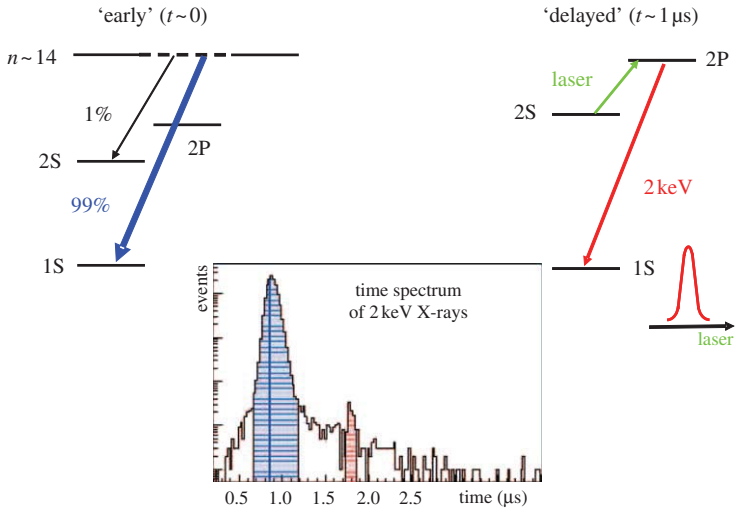

Figure 1. Principle of the muonic hydrogen experiment. Muons are stopped in 1 hPa H_2 gas; 99% undergo radiative cascade to the 1S state, producing a large early peak of 2 keV radiation. The 2S–2P transition is detected as the smaller peak owing to the laser-induced X-rays, at the time of the laser arrival (approx. 0.7 μs) to the muon stop volume. (Online version in colour.)

This cascade has been carefully studied [28], especially the collisional quenching of the 2S state [29–31]. Ninety-nine per cent of atoms decay to the 1S state, producing a large 2 keV fluorescence early peak. About 1 per cent of muonic hydrogen is formed in the long-lived 2S state [32]. A laser pulse triggered by muons (see below) is sent into the H_2 target. Because of the short delay between the laser trigger and the output of the laser, a time-delayed 2 keV fluorescence peak is observed if the 2S–2P transition has been excited by the 6 μm light.

(*b*) *Apparatus*

The challenges of the muonic hydrogen experiment were the production of long-lived muonic hydrogen in the 2S state, the development of the 6 μm laser that can be randomly triggered with a short delay and the analysis of the small signal produced (few counts/hours).

To reduce collisional quenching of the 2S state, muons are stopped in H_2 gas at a pressure of 1 hPa. To do this, a special low-energy muon beam (approx. keV) has been designed and built at the Paul Scherrer Institute to efficiently stop muons at this ultra-low gas pressure within the small target volume required for efficient laser excitation. At 1 hPa, the lifetime of the 2S metastable state is around 1 μs [29,30]. Many details of this muon line can be found in [28,33–37]. We want to emphasize that a lot of effort has been put into the quality of the signal triggering the laser. The detection of keV-muons without stopping them is not a simple task. It is done with a thin carbon foil stack which simultaneously acts as the muon detector and improves the beam quality by frictional cooling [38].

The design of the laser is dictated by the need for a tunable light source at 6 μm that can be triggered within 1 μs after a random trigger by incoming muons. The laser chain used in the 2009 run derived from development of the initial laser

http://doc.rero.ch

chain used in 2003 [34]. The fast and powerful pulsed laser that can be triggered at 515 nm is used to pump an oscillator–amplifier titanium sapphire (TiSa) laser. Three consecutive vibrational Raman scatterings in H_2 in a multiple-pass cell are used to convert the 708 nm light into a 6 μm pulse. The 6 μm light is then sent, 20 m away, in a specially design multi-pass non-resonant cavity surrounding the H_2 target in which μ-p atoms are formed. The latter cavity is used to illuminate all the stopping volume of the muon in the target ($5 \times 15 \times 190\,\mathrm{mm}^3$). The frequency of the 6 μm light is driven by the TiSa oscillator, which is seeded by a cw-TiSa laser. The frequency of the cw-laser is permanently controlled with two wavemetres, a very stable Fabry–Perot cavity and atomic/molecular lines (I_2, Cs, Rb). The cw-laser is permanently locked on a Fabry–Perot fringe. The step of scanning the laser frequency is a multiple of the free spectral range of this Fabry–Perot interferometer [39]. Whereas the design of the TiSa ensemble has remained the same between the first and the last runs [40], the design of the green pump laser has had to be changed drastically. A thin disc laser had to be built specially for our experiment [41].

The analysis of small signal requires very good knowledge of the background. Since the early stages of the experiment, the 2 keV detectors (large area avalanche photodiodes) have been well studied in order to maximize their time and energy resolutions [35,36,42]. During the data analysis, background events were efficiently rejected. The final rate of about one background event per hour originated mainly from electrons from muon decay which were wrongly identified as 2 keV Lyman-α X-rays.

(*c*) *Results*

Many muonic hydrogen lines were observed during the fourth beam time period. The first line which was observed and analysed was the most intense one: $2S_{1/2}(F=1)$–$2P_{3/2}(F=2)$ of muonic hydrogen (figure 2). The signal is clearly visible above the noise. A total of 550 events were measured in the resonance, where 155 background events were expected. A Lorentzian profile has been fitted to the data to give the frequency of the line versus the Fabry–Perot fringe. The absolute frequency of the line is determined from the absolute calibration of the light at 6 μm using the well-known H_2O spectroscopy and the free spectral range of the Fabry–Perot interferometer (figure 3). A careful and detailed analysis of the uncertainty budget of the centroid position of this line has been done in Nebel [37] and Pohl *et al.* [39].

The quantity determined by our experiment is the absolute frequency of the $2S_{1/2}(F=1)$–$2P_{3/2}(F=2)$ resonance of muonic hydrogen: 49 881.88(76) GHz. The main contribution to the uncertainty is statistical; it is given by the fit of the Lorentzian shape on the experimental data. The relative uncertainty of the centroid position (1.6×10^{-5}) corresponds to 4 per cent of the line width (approx. 18 GHz), which shows that our experiment is far away from a high-resolution spectroscopy one but which also indicates a very weak dependence of the centroid of the resonance on the line shape model.

Nevertheless, the present result is good enough to extract the proton radius with the smallest uncertainty to date. The value of the proton radius is obtained from the comparison of our determination of the frequency of the $2S_{1/2}$ $(F=1)$–$2P_{3/2}(F=2)$ muonic line with the theoretical prediction. The theoretical

http://doc.rero.ch

http://doc.rero.ch

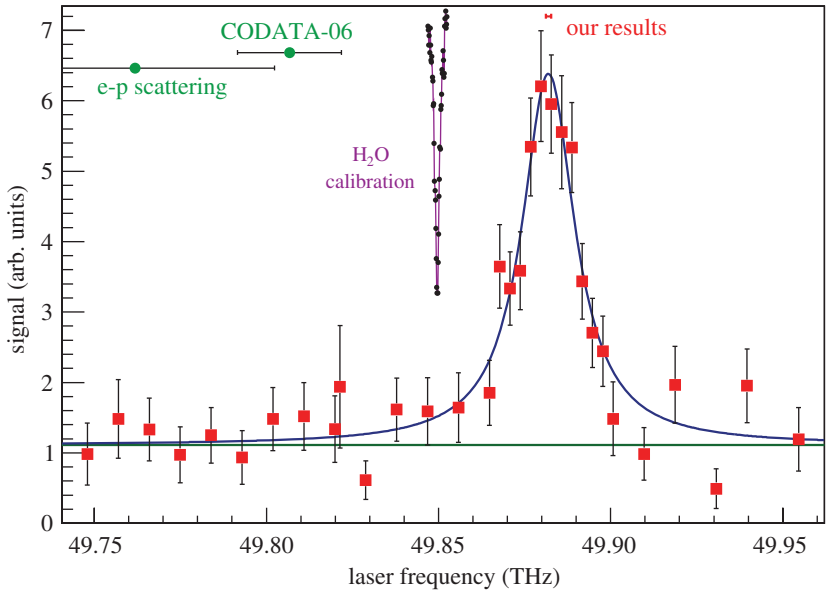

Figure 2. $2S_{1/2}(F=1)$–$2P_{3/2}(F=2)$ resonance. The discrepancy with other determinations is clearly visible. The frequency gap is around 75 GHz with the position of the line expected with electronic hydrogen. The inset calibration H_2O line was recorded at 30 hPa. (Online version in colour.)

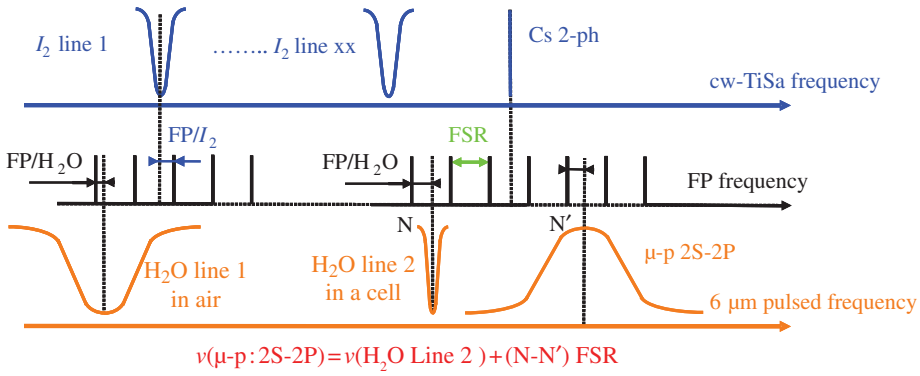

Figure 3. Principle of the determination of the absolute frequency of the muonic hydrogen line. The absolute calibration has been made with five H_2O lines, 17 I_2 lines, five Cs two-photon atomic lines and three Rb lines. Absolute calibration between 5.49 μm and 6.04 μm was performed with H_2O lines with the pulsed laser source while the free spectral range of the Fabry–Perot interferometer was determined in the cw regime in the 695–780 nm range with well-known atomic/molecular lines. To detect an eventual drift of the Fabry–Perot interferometer, this was regularly compared with iodine lines before, during and after the beam time. The integer numbers (N,N′) can be determined accurately using the two wavemetres. (Online version in colour.)

prediction derives for a large part from the bound state QED of electronic hydrogen scaled with the mass of the muon. These predictions account for radiative, recoil, proton structure fine and hyperfine contributions. A detailed

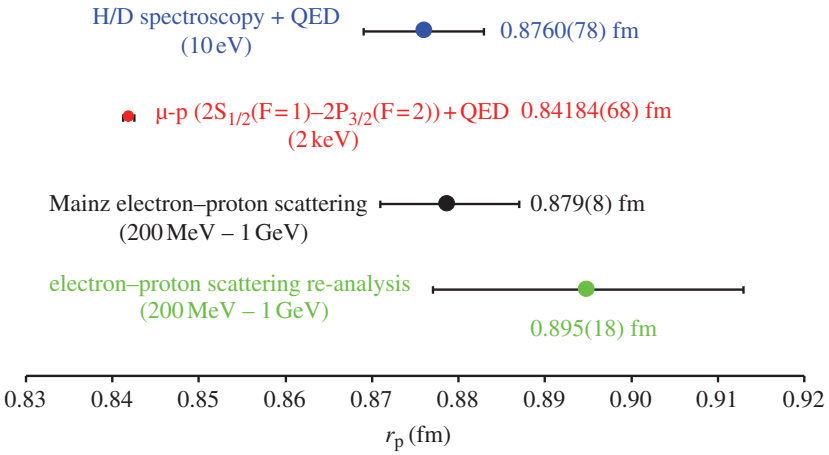

Figure 4. Comparison of the various determinations of the proton radius. Defining the proton radius as the slope of the Sachs form factor, experimental results are sorted from low-momentum transfer (electronic hydrogen) to high-momentum transfer (scattering experiments) [44]. This presentation emphasizes the surprising result of muonic hydrogen, which can be viewed as a 'dip in the form factor slope' at the corresponding Q^2 momentum of the muonic hydrogen experiment. (Online version in colour.)

http://doc.rero.ch

list of the contributions can be found in Pohl *et al.* [43]. The predicted frequency of the $2S_{1/2}(F=1)$–$2P_{3/2}(F=2)$ transition of muonic hydrogen is

$$\nu(\mathrm{GHz}) = 50772.43(1.18) - 1263.69 \times r_p^2 + 8.39 \times r_p^3. \tag{3.1}$$

The deduced value of r_p is 0.84184(36)(56) fm, where the first and second uncertainty originate, respectively, from experimental uncertainty and theoretical uncertainty. This result (0.84184(68) fm) differs significantly (approx. 5 s.d.) from other determinations (figure 4).

4. The proton radius puzzle

The confusing situation about r_p is known as the proton radius puzzle. It has stimulated intense activity in the community. It is impossible to make an exhaustive list of all the contributions already available on the arxiv base; we apologize to authors whose papers are not cited. We can only point out some of the searches at the present date.

(*a*) *Definition of the proton radius*

An obvious concern in the comparison is to make sure that the proton radius extracted from various experiments has the same meaning. The first positive answer was given in Jentschura [45]: 'a conceivable accidental incompatibility of

the conventions used in references [...] for the proton radius therefore cannot be the reason for the observed discrepancy', where [...] refers to all the proton radius determinations.

(*b*) *Charge distribution in the proton*

The charge radius distribution is related to G_E by the Fourier transformation. One attempt has been made to re-evaluate the third Zemach moment of the proton [46] $\langle r_{\mathrm{p}}^3 \rangle$ to solve the proton radius puzzle. However, the re-evaluation of $\langle r_{\mathrm{p}}^3 \rangle$ with the charge distribution presented in De Rujula [47] is in contradiction to the electron–proton scattering data [48,49].

(*c*) *Quantum electrodynamics corrections*

The contradiction between the proton radius extracted from electronic hydrogen and that from muonic hydrogen is intriguing for QED specialists. Because of the mass scaling law, the QED of muonic hydrogen has always been considered to be simpler than that of the hydrogen atom. Nevertheless, the proton radius puzzle has stimulated either careful checks of present QED corrections or evaluation of new corrections for hydrogen atoms [50–52]. Up to now, the proton radius puzzle cannot be solved with new or wrong QED corrections.

(*d*) *Rydberg constant*

The Rydberg constant is the scaling factor of the atomic level. Assuming the correctness of the QED calculations in the electronic hydrogen atom, the problem can be solved by shifting by 5 s.d. the value of the Rydberg constant, known with an uncertainty of 22 kHz, using the most accurate frequency measured in hydrogen [23]. However, the CODATA Rydberg constant is determined not only with 1S–2S and 2S–8S frequency transitions but also with other frequency measurements that are certainly less accurate but that are all highly consistent with each other and with theory [3]. Moreover, the recent measurement of the 1S–3S transition in hydrogen [53] is in very good agreement with the theoretical estimate [54]. At the present time, there are no indications of a disagreement between theory and experiments in electronic hydrogen. But it is clear that the accuracy of the hydrogen experiments other than the 1S–2S one has to be improved to clarify the situation. Figure 5 shows all the values of r_{p} deduced from the 1S–2S transition frequency, the $1/n^3$ law and only one of the 2S–n(S,P,D) transition frequencies that have been measured. Individually, there is not a large discrepancy with the muonic determination of r_{p}. On the other hand, most of the values are pointing in the same direction.

Many ongoing experiments are being carried out to test the bound state QED. Results for the 2S–6S/D transitions measured at the National Physical Laboratory [62], which are currently being analysed, may bring an important and independent contribution to the hydrogen spectroscopy and so to the proton radius puzzle. Combined with the ongoing experiment at Garching, which is aimed at measuring the 1S–2S transition in He^+ [63], the experiment planned at the Paul Scherrer Institute to measure the muonic helium ion Lamb shift ($\mu\mathrm{He}^+$) may illuminate the proton radius conundrum [64]. A determination of the

http://doc.rero.ch

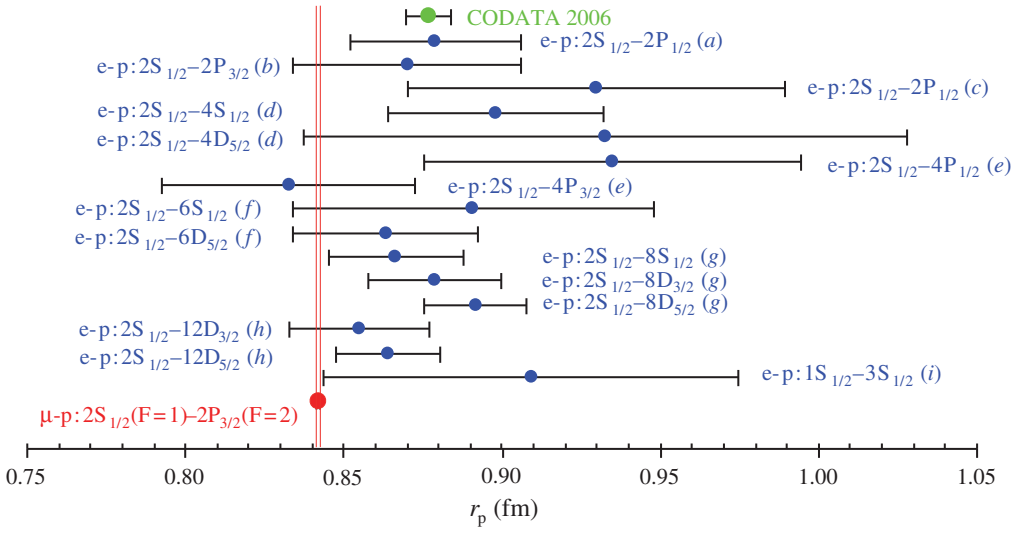

Figure 5. Comparison of various determinations of the proton radius from hydrogen spectroscopy. Each value is obtained from the 1S–2S transition frequency, the $1/n^3$ law and one of the other hydrogen experimental data from 2S–n(S,P,D). ((*a*) From Lundeen & Pipkin [55], (*b*) from Hagley & Pipkin [56], (*c*) from Newton *et al.* [57], (*d*) from Weitz *et al.* [58], (*e*) from Berkeland *et al.* [59], (*f*) from Bourzeix *et al.* [60] combined with Arnoult *et al.* [53], (*g*) from de Beauvoir *et al.* [24], (*h*) from Schwob *et al.* [61], and (*i*) from Arnoult *et al.* [53]). The double line corresponds to the uncertainty of the proton radius determination obtained from muonic hydrogen spectroscopy. (Online version in colour.)

Rydberg constant nearly independent of the nucleus structure has also started at NIST Gaithersburg, with the study of circular states of $^{20}Ne^{9+}$ [65].

(*e*) *New physics*

A possible way to solve the proton radius puzzle would be to introduce new 'particles' which are coupled differently to the muon compared with the electron. However, this new physics search is already constrained by many low-energy data [44,66,67]. Indeed, for example, recent laboratory-sized experiments are sufficiently accurate to set a limit on the internal structure of the electron or on the existence of new dark matter particles assuming the exactness of QED calculations or testing for the first time the muon and hadron contributions to the electron anomaly a_e [68,69]. A deviation from Coulomb's Law in muonic hydrogen is also ruled out by measurements in electronic hydrogen [70].

5. The proton and the redefinition of the International System of Units

As discussed above, the new determination of the proton radius may affect the value of the Rydberg constant R_∞. This constant is related to many fundamental constants. For example, the estimate of the mass of the electron m_e in the CODATA adjustment is derived from the relation

$$m_e = \frac{2R_\infty h}{c\alpha^2}, \tag{5.1}$$

http://doc.rero.ch

where α is the fine structure constant, c is the velocity of light and h is the Planck constant. The Rydberg constant also links the two ways proposed for the redefinition of the kilogram, the Avogadro constant N_{A} and the Planck constant h,

$$N_{\mathrm{A}} \times h = \frac{c}{2} \frac{A_e \alpha^2 M_u}{R_\infty}. \tag{5.2}$$

However, the current relative uncertainty on the experimental determinations of N_{A} [71] or h [72] is of the order of a few parts of 10^8. This is three orders of magnitude larger than the 'possible' shift of the Rydberg constant that may be disclosed by the new value of the proton size radius from muonic hydrogen. The proton radius puzzle will not interfere in the redefinition of the kilogram.

For many years, the hydrogen atom has been advocated as an 'ideal' clock (e.g. [73]) as, in principle, it can be calculated in contrary to the other clocks. Should the second be redefined by the hydrogen atom in terms of fundamental constants? Today, calculations for hydrogen are about 10 000 times less accurate than current experimental caesium clock precision, owing to the growing complexity of the calculations of higher order corrections. The best experimental determination is also 10^3 times worse than the best optical clocks, which are front-runners to redefining the second in several years' time (see Gill [74]). Improved theory with higher order corrections to two or three more orders is needed before the calculable clock approach for hydrogen becomes competitive.

Nevertheless, finding the solution of the proton radius puzzle would be a step in the long quest to decode the hydrogen spectrum: the 'Rosetta stone of modern physics' [75].

References

1 Dürr, S. *et al.* 2008 *Ab initio* determination of light hadron masses. *Science* **322**, 1224–1227. (doi:10.1126/science.1163233)

2 Alexandrou, C. *et al.* 2008 Light baryon masses with dynamical twisted mass fermions. *Phys. Rev. D.* **78**, 014509. (doi:10.1103/PhysRevD.78.014509)

3 Mohr, P. J., Taylor, B. N. & Newell, D. B. 2008 CODATA recommended values of the fundamental physical constants: 2006. *Rev. Mod. Phys.* **80**, 633–730. (doi:10.1103/RevModPhys.80.633)

4 Thomas, A. W. 2008 The spin of the proton. *Prog. Part. Nucl. Phys.* **61**, 219–228. (doi:10.1016/j.ppnp.2007.12.039)

5 Ashman, J. *et al.* 1988 A measurement of the spin asymetry and determination of the structure function g1 in deep inelastic muon-proton scattering. *Phys. Lett. B* **206**, 364–370. (doi:10.1016/0370-2693(88)91523-7)

6 Aubert, J. J. *et al.* 1985 A detailed study of the proton structure functions in deep inelastic muon–proton scattering. *Nucl. Phys. B* **259**, 189–265. (doi:10.1016/0550-3213(85)90635-2)

7 Leader, E. & Anselmino, M. 1988 A crisis in the parton model: where, oh where is the proton's spin? *Z. Phys. C Part. Fields* **41**, 239–246. (doi:10.1007/BF01566922)

8 Vogelsang, W. 2009 QCD spin physics: theoretical overview. *Nucl. Phys. A* **827**, 110c–117c. (doi:10.1016/j.nuclphysa.2009.05.025)

9 Hasch, D. 2009 Spin physics: experimental overview. *Nucl. Phys. A* **827**, 101c–109c. (doi:10.1016/j.nuclphysa.2009.05.024)

10 Leinweber, D. B. & Cohen, T. D. 1993 Chiral corrections to lattice calculations of charge radii. *Phys. Rev. D* **47**, 2147–2150. (doi:10.1103/PhysRevD.47.2147)

11 Wang, P., Leinweber, D. B., Thomas, A. W. & Young, R. D. 2009 Chiral extrapolation of octet-baryon charge radii. *Phys. Rev. D* **79**, 094001. (doi:10.1103/PhysRevD.79.094001)

http://doc.rero.ch

12 Hofstadter, R. & McAllister, R. 1955 Electron scattering from the proton. *Phys. Rev.* **98**, 217–218. (doi:10.1103/PhysRev.98.217)
13 Simon, G. G., Schmitta, Ch., Borkowskia, F. & Walthera, V. H. 1980 Absolute electron-proton cross sections at low momentum transfer measured with a high pressure gas target system. *Nucl. Phys. A* **333**, 381–391. (doi:10.1016/0375-9474(80)90104-9)
14 Hand, L. N. *et al.* 1963 Electric and magnetic form factors of the nucleon. *Rev. Mod. Phys.* **35**, 355–349. (doi:10.1103/RevModPhys.35.335)
15 Mergell, P., Meißner, U.-G. & Drechsel, D. 1996 Dispersion-theoretical analysis of the nucleon electromagnetic form factors. *Nucl. Phys. A* **596**, 367–396. (doi:10.1016/0375-9474(95)00339-8)
16 Borisyuk, D. 2010 Proton charge and magnetic rms radii from the elastic ep scattering data. *Nucl. Phys. A* **843**, 59–67. (doi:10.1016/j.nuclphysa.2010.05.054)
17 Sick, I. 2003 On the rms-radius of the proton. *Phys. Lett. B* **576**, 62–67. (doi:10.1016/j.physletb.2003.09.092)
18 Bernauer, J. C. 2010 Measurement of the elastic electron–proton cross section and separation of the electric and magnetic form factor in the Q^2 range from 0.004 to 1 $(GeV/c)^2$. PhD thesis, Johannes Gutenberg-Universität Mainz. (http://ubm.opus.hbz-nrw.de/volltexte/2010/2442/).
19 Bernauer, J. C. *et al.* 2010 High-precision determination of the electric and magnetic form factors of the proton. *Phys. Rev. Lett.* **105**, 242001. (doi:10.1103/PhysRevLett.105.242001)
20 Zhan, X. *et al.* 2011 High precision measurement of the proton elastic form factor ratio $\mu p G_E/G_M$ at low Q^2. (http://arxiv:1102.0318v1 [nucl-ex]).
21 Arrington, J., Melnitchouk, W. & Tjon, J. A. 2007 Global analysis of proton elastic form factor data with two-photon exchange corrections. *Phys. Rev. C* **76**, 035205. (doi:10.1103/PhysRevC.76.035205)
22 de Beauvoir, B., Schwob, C., Acef, O., Jozefowski, L., Hilico, L., Nez, F., Julien, L., Clairon, A. & Biraben, F. 2000 Metrology of the hydrogen and deuterium atoms: determination of the Rydberg constant and Lamb shifts. *Eur. Phys. J. D* **12**, 61–93. (doi:10.1007/s100530070043)
23 Niering, N. *et al.* 2000 Measurement of the Hydrogen 1S–2S transition frequency by phase coherent comparison with a microwave cesium fountain clock. *Phys. Rev. Lett.* **84**, 5496–5499. (doi:10.1103/PhysRevLett.84.5496)
24 de Beauvoir, B. *et al.* 1997 Absolute frequency measurement of the 2S–8S/D transitions in hydrogen and deuterium: new determination of the Rydberg constant. *Phys. Rev. Lett.* **78**, 440–443. (doi:10.1103/PhysRevLett.78.440)
25 Karsenboim, S. G. J. 1996 Two-loop logarithmic corrections in the hydrogen Lamb shift. *Phys. B* **29**, L29. (doi:10.1088/0953-4075/29/2/001)
26 Czarnecki, A., Jentschura, U. D. & Pachucki, K. 2005 Calculation of the one- and two-loop lamb shift for arbitrary excited hydrogenic states. *Phys. Rev. Lett.* **95**, 180404. (doi:10.1103/PhysRevLett.95.180404)
27 Pohl, R. *et al.* 2011 The Lamb shift in muonic hydrogen. *Can. J. Phys.* **89**, 37.
28 Pohl, R. 2001 Investigation of the long-lived metastable 2S state in muonic hydrogen. PhD thesis, ETH Zurich, Switzerland. (http://e-collection.ethbib.ethz.ch/view/eth23936).
29 Pohl, R. *et al.* 2001 Observation of molecular quenching of μp(2S) atoms. *Hyperfine Interact.* **138**, 35–40. (doi:10.1023/A:1020830229258)
30 Pohl, R. *et al.* 2006 Observation of long-lived muonic hydrogen in the 2S state. *Phys. Rev. Lett.* **97**, 193402. (doi:10.1103/PhysRevLett.97.193402)
31 Ludhova, L. *et al.* 2007 Muonic hydrogen cascade time and lifetime of the short-lived 2S state. *Phys. Rev. A* **75**, 040501. (doi:10.1103/PhysRevA.75.040501)
32 Pohl, R. 2009 2S state and Lamb shift in muonic hydrogen. *Hyperfine Interact.* **193**, 115–120. (doi:10.1007/s10751-009-0054-1)
33 Antognini, A. *et al.* 2005 The 2S lamb shift in muonic hydrogen and the proton rms charge radius. *AIP Conf. Proc.* **796**, 253–259. (doi:10.1063/1.2130175)
34 Antognini, A. 2005 The lamb shift experiment in muonic hydrogen. PhD thesis, LMU Munich, Germany. (http://edoc.ub.uni-muenchen.de/5044/).
35 Ludhova, L. 2005 The muonic hydrogen Lamb shift experiment: lifetime and population of the μp($2S$) state. PhD thesis, University of Fribourg, Switzerland. (http://ethesis.unifr.ch/theses/downloads.php).

http://doc.rero.ch

36 Fernandes, L. M. P. 2006 Characterization of large area avalanche photodiodes for detection of X-rays, vacuum ultraviolet and visible light. PhD thesis, University of Coimbra, Portugal. (http://gian.fis.uc.pt/theses/lmpf/phd2005.pdf).
37 Nebel, T. 2010 The Lamb shift in muonic hydrogen: Die Lamb-Verschiebung in myonischem Wasserstoff. PhD thesis, LMU Munich, Germany. (http://edoc.ub.uni-muenchen.de/12094/).
38 Muhlbauer, M., Daniel, H., Hartmann, F. J., Hauser, P., Kottmann, F., Petitjean, C., Schott, W., Taqqu, D. & Wojciechowski, P. 1999 Frictional cooling: experimental results. *Hyperfine Interact.* **119**, 305–310. (doi:10.1023/A:1012624501134)
39 Pohl, R. *et al.* 2010 The size of the proton. *Nature* **466**, 213–216. (doi:10.1038/nature09250)
40 Antognini, A. *et al.* 2005 Powerful fast triggerable 6 micrometer laser for the muonic hydrogen 2S–Lamb shift experiment. *Opt. Comm.* **253**, 362–374. (doi:10.1016/j.optcom.2005.04.079)
41 Antognini, A. *et al.* 2009 Thin-disk Yb:YAG oscillator–amplifier laser, ASE, and effective Yb:YAG lifetime. *IEEE J. Quantum Electron.* **45**, 993–1005. (doi:10.1109/JQE.2009.2014881)
42 Ludhova, L. *et al.* 2005 Planar LAAPDs: temperature dependence, performance, and application in low energy X-ray spectroscopy. *Nucl. Instrum. Methods A* **540**, 169–179. (doi:10.1016/j.nima.2004.11.017)
43 Pohl, R. *et al.* 2010 2S-2P splitting in muonic hydrogen. *Nature* **466**, 213–216 (supplementary informations).
44 Jentschura, U. 2011 Lamb shift in muonic hydrogen. II. Analysis of the discrepancy of theory and experiment. *Ann. Phys.* **326**, 516–533. (doi:10.1016/j.aop.2010.11.011)
45 Jentschura, U. 2011 Proton radius, Darwin–Foldy term and radiative corrections. *Eur. Phys. J. D* **61**, 7–14. (doi:10.1140/epjd/e2010-10414-6)
46 Friar, J. L. & Sick, I. 2005 Muonic hydrogen and the third Zemach moment. *Phys. Rev. A* **72**, 040502. (doi:10.1103/PhysRevA.72.040502)
47 De Rújula, A. 2010 QED is not endangered by the proton's size. *Phys. Lett. B* **693**, 555–558. (doi:10.1016/j.physletb.2010.08.074)
48 Distler, M. O., Bernauer, J. C. & Walcher, T. 2011 The RMS charge radius of the proton and Zemach moments. *Phys. Lett. B* **696**, 343–347. (doi:10.1016/j.physletb.2010.12.067)
49 Cloet, I. C. & Miller, G. A. 2011 Third Zemach moment of the proton. *Phys. Rev. C* **83**, 012201(R). (doi:10.1103/PhysRevC.83.012201)
50 Jentschura, U. 2011 Lamb shift in muonic hydrogen. I. Verification and update of theoretical predictions. *Ann. Phys.* **326**, 500–515. (doi:10.1016/j.aop.2010.11.012)
51 Yerokhin, V. 2011 Nuclear-size correction to the Lamb shift of one-electron atoms. *Phys Rev A* **83**, 012507. (doi:10.1103/PhysRevA.83.012507)
52 Karshenboim, S. G., Ivanov, V. G., Korzinin, E. Yu. & Shelyuto, V. A. 2010 Nonrelativistic contributions of order $\alpha^5\, m_\mu c^2$ to the Lamb shift in muonic hydrogen and deuterium, and in the muonic helium ion. *Phys. Rev. A* **81**, 060501(R). (doi:10.1103/PhysRevA.81.060501)
53 Arnoult, O., Nez, F., Julien, L. & Biraben, F. 2010. Optical frequency measurement of the 1S–3S two-photon transition in hydrogen. *Eur. Phys. J. D* **60**, 243–256. (doi:10.1140/epjd/e2010-00249-6)
54 Jentschura, U. D., Kotochigova, S., Le Bigot, E. O., Mohr, P. J. & Taylor, B. N. 2005 Precise calculation of transition frequencies of Hydrogen and deuterium based on a least-squares analysis. *Phys. Rev. Lett.* **95**, 163003. (doi:10.1103/PhysRevLett.95.163003)
55 Lundeen, S. R. & Pipkin, F. M. 1986 Separated oscillatory field measurement of the lamb shift in H, $n = 2$. *Metrologia* **22**, 9. (doi:10.1088/0026-1394/22/1/003)
56 Hagley, E. W. & Pipkin, F. M. 1994 Separated oscillatory field measurement of hydrogen $2S_{1/2}$–$2P_{3/2}$ fine structure interval. *Phys. Rev. Lett.* **72**, 1172–1175. (doi:10.1103/PhysRevLett.72.1172)
57 Newton, G., Andrews, D. A. & Unsworth, P. J. 1979 A precision determination of the lamb shift in hydrogen. *Phil. Trans. R. Soc. Lond. A* **290**, 373–404. (doi:10.1098/rsta.1979.0004)
58 Weitz, M. *et al.* 1995 Precision measurement of the 1S ground-state lamb shift in atomic hydrogen and deuterium by frequency comparison. *Phys. Rev. A* **52**, 2664–2681. (doi:10.1103/PhysRevA.52.2664)
59 Berkeland, D. J., Hinds,E. A. & Boshier, M. G. 1995 Precise optical measurement of lamb shifts in atomic hydrogen. *Phys. Rev. Lett.* **75**, 2470–2473. (doi:10.1103/PhysRevLett.75.2470)

http://doc.rero.ch

60 Bourzeix, S., de Beauvoir, B., Nez, F., Plimmer, M. D., de Tomasi, F., Julien, L., Biraben, F. & Stacey, D. N. 1996 High resolution spectroscopy of the hydrogen atom: determination of the 1S lamb shift. *Phys. Rev. Lett.* **76**, 384–387. (doi:10.1103/PhysRevLett.76.384)
61 Schwob, C. *et al.* 1999 Optical frequency measurement of the 2S–12D transitions in hydrogen and deuterium: Rydberg constant and lamb shift determinations. *Phys. Rev. Lett.* **82**, 4960–4963. (doi:10.1103/PhysRevLett.82.4960)
62 Flowers, J., Baird, P. E. G., Bougueroua, L., Klein, H. A. & Margolis, H. S. 2007 The NPL Rydberg constant experiment. *IEEE Trans. Instrum. Meas.* **56**, 331–335. (doi:10.1109/TIM.2007.890598)
63 Hermann, M. *et al.* 2009 Feasibility of coherent xuv spectroscopy on the $1S$–$2S$ transition in singly ionized helium. *Phys. Rev. A* **79**, 052505. (doi:10.1103/PhysRevA.79.052505)
64 Antognini, A. *et al.* 2011 Illuminating the proton radius conundrum: the muonic helium lamb shift. *Can. J. Phys.* **89**, 47–57. (doi:10.1139/P10-113)
65 Jentschura, U. D., Mohr, P. J., Tan, J. N. & Wundt, B. J. 2008 Fundamental constants and tests of theory in Rydberg states of hydrogenlike ions. *Phys. Rev. Lett.* **100**, 160404. (doi:10.1103/PhysRevLett.100.160404)
66 Karshenboim, S. G. 2010 Precision physics of simple atoms and constraints on a light boson with ultraweak coupling. *Phys. Rev. Lett.* **104**, 220406. (doi:10.1103/PhysRevLett.104.220406)
67 Barger, V., Chiang, C. W., Keung, W. Y. & Marfatia, D. 2011 Proton size anomaly. *Phys. Rev. Lett.* **106**, 153001. (doi:10.1103/PhysRevLett.106.153001)
68 Hanneke, D., Fogwell, S. & Gabrielse, G. 2008 New measurement of the electron magnetic moment and the fine structure constant. *Phys. Rev. Lett.* **100**, 120801. (doi:10.1103/PhysRevLett.100.120801)
69 Bouchendira, R., Cladé, P., Guellati-Khélifa, S., Nez, F. & Biraben, F. 2011 New determination of the fine structure constant and test of the quantum electrodynamics. *Phys. Rev. Lett.* **106**, 080801. (doi:10.1103/PhysRevLett.106.080801)
70 Jaeckel, J. & Roy, S. 2010 Spectroscopy as a test of Coulomb's law: a probe of the hidden sector. *Phys. Rev. D* **82**, 125020. (doi:10.1103/PhysRevD.82.125020)
71 Andreas, B. *et al.* 2011 Determination of the avogadro constant by counting the atoms in a ^{28}Si crystal. *Phys. Rev. Lett.* **106**, 030801. (doi:10.1103/PhysRevLett.106.030801)
72 Steiner, R. L., Williams, E. R., Liu, R. & Newell, D. B. 2007 Uncertainty improvements of the NIST electronic kilogram. *IEEE Trans. Instrum. Meas.* **56**, 592–596. (doi:10.1109/TIM.2007.890590)
73 Bordé, C. J. 2005 Base units of the SI, fundamental constants and modern quantum physics. *Phil. Trans. R. Soc. A* **363**, 2177–2201. (doi:10.1098/rsta.2005.1635)
74 Gill, P. 2011 When should we change the definition of the second? *Phil. Trans. R. Soc. A* **369**, 4109–4130. (doi.10.1098/rsta.2011.0237)
75 Hänsch, T. W., Schawlow, A. L. & Series, G. W. 1979 The spectrum of atomic Hydrogen. *Sci. Am.* **240**, 94–111. (doi:10.1038/scientificamerican0379-94)

http://doc.rero.ch